

Technical Memorandum 4310

H1/39

00068

p/6

Compressive Buckling Analysis of Hat-Stiffened Panel

by ~~W. Ko~~ and Raymond H. Jackson

(NASA-TM-4310) COMPRESSIVE BUCKLING
ANALYSIS OF HAT-STIFFENED PANEL (NASA)

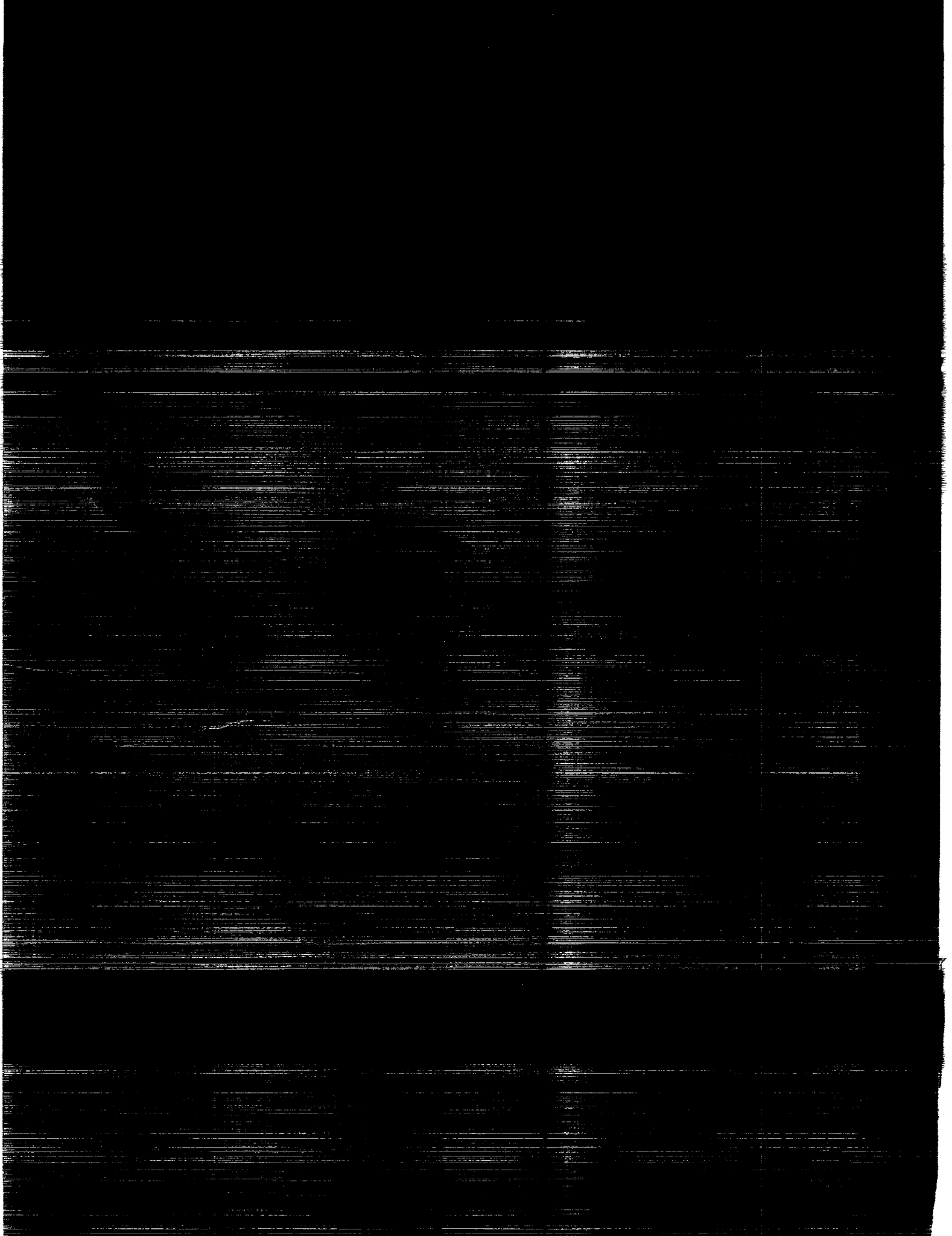
16 p

CSSL 20K

TM-4310

Unclas

H1/39 0030068



NASA Technical Memorandum 4310

Compressive Buckling Analysis of Hat-Stiffened Panel

William L. Ko and Raymond H. Jackson
Dryden Flight Research Facility
Edwards, California



National Aeronautics and
Space Administration

Office of Management

Scientific and Technical
Information Program

1991

ABSTRACT

Buckling analysis was performed on a hat-stiffened panel subjected to uniaxial compression. Both local buckling and global buckling were analyzed. It was found that the global buckling load was several times higher than the local buckling load. The predicted local buckling loads compared favorably with both experimental data and finite-element analysis.

INTRODUCTION

Various advanced hot-structural panel concepts have been investigated for applications to hypersonic aircraft wing panels (ref. 1). Among those panels investigated, the beaded panels and the tubular panels were found to be highly efficient (that is, high stiffness to weight density ratio). The buckling behavior of these two types of hot-structural panels were studied extensively, both theoretically and experimentally (refs. 2 and 3).

One of the recently developed wing panels with potential application to hypersonic aircraft is a hat-stiffened panel, as shown in figure 1. This panel is equivalent to a corrugated core sandwich panel with one face sheet removed.

This report presents a buckling analysis of the hat-stiffened panel under uniaxial compression. The predicted buckling loads are compared with the experimental data and finite-element solutions.

NOMENCLATURE

A	cross-sectional area of reinforcing edge beam that is the cross-sectional area of one corrugation leg, $A = \ell t_c$, in ²
\bar{A}	cross-sectional area of global panel segment bounded by p , $A + pt_s + \frac{1}{2}(f_1 - f_2)t_c$, in ²
a	length of global panel, in.
b	width of rectangular flat plate segment, or horizontal distance between centers of corrugation and curved region, $\frac{1}{2} \left[p - \frac{1}{2}(f_1 + f_2) \right]$, in.
c	width of global panel, in.
D	flexural rigidity of flat plate, $\frac{E_s t_s^3}{12(1 - \nu_s^2)}$, $\frac{\text{lb-in}^2}{\text{in}}$
d	one-half of diagonal region of corrugation leg, in.
E_c	modulus of elasticity of hat material, lb/in ²
E_s	modulus of elasticity of face sheet material, lb/in ²
f_1	lower flat region of hat stiffener, in.
f_2	upper flat region of hat stiffener, in.
G_c	shear modulus of hat material, lb/in ²
G_s	shear modulus of face sheet material, lb/in ²
h	distance between middle surfaces of hat top flat region and face sheet, $h_c + \frac{1}{2}(t_c + t_s)$, in.
h_c	distance between middle surfaces of hat top and bottom flat regions, in.
h_o	distance between middle surface of face sheet and centroid of global panel segment, in.
I_c	$\frac{1}{12} t_c^3$, in ⁴ /in

I_c^*	moment of inertia of corrugation leg of length ℓ (reinforcing edge beam) taken with respect to its neutral axis η , in ⁴
\bar{I}_c	moment of inertia, per unit width, of one-half of reinforcing hat taken with respect to the neutral axis η_o of the hat-stiffened panel, in ⁴ /in
I_f	$\frac{1}{12} t_s^3$, in ⁴ /in
I_s	moment of inertia, per unit width, of face sheet with respect to η_o axis passing through the centroid of the global panel segment, $t_s h_o^2 + \frac{1}{12} t_s^3$, in ⁴ /in
k_x	compressive buckling load factor, no dimension
ℓ	length of corrugation leg, $f_2 + 2d + 2R\theta$, in.
m	number of buckle half-waves in x -direction
$(N_x)_{cr}$	panel compressive buckling load, lb/in
n	number of buckle half-waves in y -direction
P	compressive load, lb
P_{cr}	compressive buckling load, lb
p	one-half of reinforcing hat pitch, in.
R	radius of circular arc segments of corrugation leg, in.
t_c	thickness of reinforcing hat, in.
t_s	thickness of face sheet, in.
x, y, z	rectangular Cartesian coordinates, in.
β	panel aspect ratio, a/c
η	neutral axis of corrugation leg
η_o	neutral axis of corrugation leg and face sheet combined
θ	corrugation angle (angle between the face sheet and the straight diagonal segment of corrugation leg), rad
ν_c	Poisson ratio of hat material
ν_s	Poisson ratio of face sheet material
σ_x	compressive stress, lb/in ²
$(\sigma_x)_{cr}$	critical compressive stress, lb/in ²

APPROACH

For analyzing the buckling behavior of the complex structure as shown in figure 1, two approaches will be taken: (1) local buckling analysis and (2) global buckling analysis (general panel instability).

Local Buckling Analysis

The local buckling analysis studies the buckling behavior of a local weak region of the panel. This weak region is identified as a rectangular flat plate region bounded by two legs of the reinforcing hat located at the center of the global panel, shown in the left diagram of figure 2. The local buckling analysis studies the buckling behavior of this rectangular flat plate (slender strip). Two types of edge conditions are considered: (1) elastically supported and (2) simply supported.

Elastically Supported

For this case, the two horizontal edges are assumed to be simply supported. The two vertical edges are supported by two elastic beams. Each of the beams has the same flexural rigidity as that of a semihat (one leg of corrugation), shown in the center diagram of figure 2.

Simply Supported

Because the reinforcing hat has high flexural rigidity, the two vertical edges of the rectangular plate are assumed simply supported, as shown in the right diagram of figure 2. Also, the two horizontal edges are assumed simply supported.

Global Buckling Analysis

In the global buckling analysis (general panel instability), the complex panel is represented by a homogeneous panel having effective elastic constants. These effective elastic constants must be calculated first. The analysis is similar to the conventional buckling analysis of sandwich panels (ref. 4).

COMPRESSIVE BUCKLING ANALYSIS

Local Buckling—Elastically Supported

The critical stress equation for a rectangular plate supported by elastic beams at its two vertical edges and subjected to uniaxial compression (ref. 5 and fig. 2) may be written as

$$\sqrt{\Psi - \phi} [\Psi + (1 - \nu_s)\phi]^2 \tan \frac{1}{2} \sqrt{\Psi \phi - \phi^2} + \sqrt{\Psi + \phi} [\Psi - (1 - \nu_s)\phi]^2 \tanh \frac{1}{2} \sqrt{\Psi \phi + \phi^2} = 2 \phi^{\frac{3}{2}} \Psi \xi \quad (1)$$

where

$$\phi = \frac{m\pi b}{a} \quad (2)$$

$$\Psi = b \sqrt{\frac{t_s \sigma_{cr}}{D}} \quad (3)$$

$$\xi = \frac{E_s I_c^*}{bD} - \frac{A \Psi^2}{bt_s \phi^2} \quad (4)$$

where

$$D = \frac{E_s t_s^3}{12(1 - \nu_s^2)} \quad (5)$$

$$A = \ell t_c = (f_2 + 2d + 2R\theta)t_c \quad (6)$$

and I_c^* is the moment of inertia of a corrugation leg of length ℓ , taken with respect to its neutral axis η (fig. 3), and is given by

$$I_c^* = h_c^3 t_c \left\{ \frac{1}{4} \frac{f_2}{h_c} \left(1 + \frac{1}{3} \frac{t_c^2}{h_c^2} \right) + \frac{2}{3} \frac{d^3}{h_c^3} \left(\sin^2 \theta + \frac{1}{4} \frac{t_c^2}{d^2} \cos^2 \theta \right) + \frac{R}{h_c} \left[\frac{\theta}{2} - \frac{R^2}{h_c^2} \sin \theta (1 - \cos \theta) - \frac{R}{h_c} \left(2 - 3 \frac{R}{h_c} \right) (\theta - \sin \theta) \right] \right\} \quad (7)$$

The panel buckling load $(N_x)_{cr}$ may then be obtained from

$$(N_x)_{cr} = (\sigma_x)_{cr} \frac{\bar{A}}{p} \quad (8)$$

where \bar{A} is the cross-sectional area of the panel segment bounded by one-half of the corrugation pitch p (fig. 3), and is given by

$$\bar{A} = A + pt_s + \frac{1}{2}(f_1 - f_2)t_c \quad (9)$$

Local Buckling—Simply Supported

The critical stress $(\sigma_x)_{cr}$ for the rectangular plate under uniaxial compression with four edges simply supported (ref. 5) may be written as

$$(\sigma_x)_{cr} = \frac{\pi^2 D}{t_s a^2} \left(m + \frac{n^2 a^2}{m b^2} \right)^2 \quad (10)$$

The panel buckling load $(N_x)_{cr}$ can then be obtained from equation (8).

Global Buckling—General Panel Instability

The current hat-stiffened panel is equivalent to a corrugated-core sandwich panel with one face sheet removed. Thus, the buckling analysis of a corrugated-core sandwich panel (ref. 4) may be applied to the present problem with slight modifications of the effective elastic constants. The compressional panel buckling load $(N_x)_{cr}$ may be obtained from the following buckling equation (ref. 4):

$$k_x = \frac{c^2 (N_x)_{cr}}{\pi^2 E_s I_s} \quad (11)$$

$$= \frac{a_{11}(a_{23}a_{32} - a_{22}a_{33}) + a_{21}(a_{12}a_{33} - a_{13}a_{32})}{a_{12}a_{23} - a_{22}a_{13}}$$

where the coefficients a_{ij} (where $i, j = 1, 2, 3$) are defined as follows:

$$a_{11} = \frac{m}{\beta} \left[\frac{1}{1 - \nu_s^2} \frac{D_x}{E_s I_s} \frac{m^2}{\beta^2} + \left(\frac{\nu_s}{1 - \nu_s^2} \frac{D_x}{E_s I_s} + \frac{D_{xy}}{E_s I_s} \right) n^2 \right] \quad (12)$$

$$a_{12} = - \left[1 + \frac{\pi^2 E_s I_s}{c^2 D_{Qx}} \left(\frac{1}{1 - \nu_s^2} \frac{D_x}{E_s I_s} \frac{m^2}{\beta^2} + \frac{1}{2} \frac{D_{xy}}{E_s I_s} n^2 \right) \right] \quad (13)$$

$$a_{13} = - \frac{\pi^2 E_s I_s}{c^2 D_{Qy}} \left(\frac{\nu_s}{1 - \nu_s^2} \frac{D_x}{E_s I_s} + \frac{1}{2} \frac{D_{xy}}{E_s I_s} \right) \frac{mn}{\beta} \quad (14)$$

$$a_{21} = n \left[\frac{1}{1 - \nu_s^2} \frac{D_y}{E_s I_s} n^2 + \left(\frac{\nu_s}{1 - \nu_s^2} \frac{D_y}{E_s I_s} + \frac{D_{xy}}{E_s I_s} \right) \frac{m^2}{\beta^2} \right] \quad (15)$$

$$a_{22} = - \frac{\pi^2 E_s I_s}{c^2 D_{Qx}} \left(\frac{\nu_s}{1 - \nu_s^2} \frac{D_y}{E_s I_s} + \frac{1}{2} \frac{D_{xy}}{E_s I_s} \right) \frac{mn}{\beta} \quad (16)$$

$$a_{23} = - \left[1 + \frac{\pi^2 E_s I_s}{c^2 D_{Qy}} \left(\frac{1}{1 - \nu_s^2} \frac{D_y}{E_s I_s} n^2 + \frac{1}{2} \frac{D_{xy}}{E_s I_s} \frac{m^2}{\beta^2} \right) \right] \quad (17)$$

$$a_{32} = - \frac{\beta}{m} \quad (18)$$

$$a_{33} = - \frac{\beta^2}{m^2} n \quad (19)$$

where

$$D_x = E_c \bar{I}_c + E_s I_s \quad (20)$$

$$D_y = E_s I_s \frac{1 + \frac{E_c \bar{I}_c}{E_s I_s}}{1 + (1 - \nu_s^2) \frac{E_c \bar{I}_c}{E_s I_s}} \quad (21)$$

$$I_s = t_s h_o^2 + \frac{1}{12} t_s^3 \quad (22)$$

and \bar{I}_c is the moment of inertia of the corrugation leg and face sheet combined, taken with respect to neutral axis η_o (fig. 3):

$$\bar{I}_c = \frac{I_c^*}{p} + \frac{A}{p} \left[\frac{1}{2} (h_c + t_c + t_s) - h_o \right]^2 + \frac{1}{24p} (f_1 - f_2) t_c^3 + \frac{f_1 - f_2}{2p} t_c \left(h_o - \frac{t_c + t_s}{2} \right)^2 \quad (23)$$

where h_o is the distance between the middle surface of the face sheet and the centroid of the global panel segment:

$$h_o = \frac{1}{2A} \left[A(h_c + t_c + t_s) + \frac{1}{2} t_c (f_1 - f_2) (t_c + t_s) \right] \quad (24)$$

and D_{xy} appearing in a_{ij} may be obtained from reference 6 with slight modification to fit the present problem in the following form:

$$D_{xy} = 2 \overline{GJ} \quad (25)$$

where

$$\overline{GJ} = \left[G_s t_s k_{GJ}^2 + \frac{p G_c t_c^2}{A_c} (k_{GJ} - k_c)^2 \right] h^2 \quad (26)$$

where

$$k_{GJ} = \frac{k_c}{1 + \frac{A_c G_s t_s}{p G_c t_c}} \quad (27)$$

and

$$k_c = \frac{1}{2} \left[1 - \frac{(f_1 - f_2) h_c}{2 p h} \right] \quad (28)$$

$$A_c = \left[\ell + \frac{1}{2} (f_1 - f_2) \right] t_c \quad (29)$$

and

$$D_{Qx} = \frac{G_c t_c h^2}{p \ell} \quad (30)$$

$$D_{Qy} = \bar{S} h \frac{E_c}{1 - \nu_c^2} \left(\frac{t_c}{h_c} \right)^3 \quad (31)$$

where

$$\bar{S} = \frac{6 \frac{h_c}{p} D_z^F \frac{t_s}{t_c} + \left(\frac{p}{h_c} \right)^2}{12 \left\{ \frac{h}{h_c} \frac{p}{h_c} D_z^F - 2 \left(\frac{p}{h_c} \right)^2 D_z^H + \frac{h_c}{h} \left[6 \frac{t_s}{t_c} (D_z^F D_y^H - D_z^H{}^2) + \left(\frac{p}{h_c} \right)^3 D_y^H \right] \right\}} \quad (32)$$

where

$$\begin{aligned} D_z^F = & \frac{2}{3} \left(\frac{d}{h_c} \right)^3 \cos^2 \theta + \frac{2}{3} \frac{I_c}{I_f} \left[\frac{1}{8} \left(\frac{p}{h_c} \right)^3 - \left(\frac{b}{h_c} \right)^3 \right] \\ & + \frac{R}{h_c} \left[2 \left(\frac{b}{h_c} \right)^2 \theta - 4 \frac{Rb}{h_c^2} (1 - \cos \theta) + \left(\frac{R}{h_c} \right)^2 (\theta - \sin \theta \cos \theta) \right] \\ & + \frac{I_c}{h_c^2 t_c} \left[2 \frac{d}{h_c} \sin^2 \theta + \frac{R}{h_c} (\theta - \sin \theta \cos \theta) \right] \end{aligned} \quad (33)$$

$$\begin{aligned} D_z^H = & \frac{2}{3} \left(\frac{d}{h_c} \right)^3 \sin \theta \cos \theta + \frac{1}{2} \frac{I_c}{I_f} \left[\frac{1}{4} \left(\frac{p}{h_c} \right)^2 - \left(\frac{b}{h_c} \right)^2 \right] \\ & + \frac{R}{h_c} \left\{ \frac{b}{h_c} \theta - 2 \frac{Rb}{h_c^2} (\theta - \sin \theta) - \frac{R}{h_c} (1 - \cos \theta) \left[1 - \frac{R}{h_c} (1 - \cos \theta) \right] \right\} \\ & - \frac{I_c}{h_c^2 t_c} \left(2 \frac{d}{h_c} \sin \theta \cos \theta + \frac{R}{h_c} \sin^2 \theta \right) \end{aligned} \quad (34)$$

$$\begin{aligned} D_y^H = & \frac{2}{3} \left(\frac{d}{h_c} \right)^3 \sin^2 \theta + \frac{1}{2} \left(\frac{R}{h_c} \theta + \frac{1}{2} \frac{f}{h_c} \frac{I_c}{I_f} \right) \\ & - \left(\frac{R}{h_c} \right)^2 \left[\left(2 - 3 \frac{R}{h_c} \right) (\theta - \sin \theta) + \frac{R}{h_c} \sin \theta (1 - \cos \theta) \right] \\ & + \frac{I_c}{h_c^2 t_c} \left[\frac{f}{h_c} \frac{t_c}{t_f} + 2 \frac{d}{h_c} \cos^2 \theta + \frac{R}{h_c} (\theta + \sin \theta \cos \theta) \right] \end{aligned} \quad (35)$$

where

$$f = \frac{1}{2} (f_1 + f_2) \quad (36)$$

$$I_c = \frac{1}{12} t_c^3 \quad (37)$$

$$I_f = \frac{1}{12} t_s^3 \quad (38)$$

$$b = \frac{1}{2} \left[p - \frac{1}{2} (f_1 + f_2) \right] \quad (39)$$

NUMERICAL RESULTS

The titanium hat-stiffened panel has the following material properties and geometries:

$$E_s = E_c = 16 \times 10^6 \text{ lb/in}^2$$

$$G_s = G_c = 6.2 \times 10^6 \text{ lb/in}^2$$

$$\nu_s = \nu_c = 0.31$$

$$a = 24 \text{ in.}$$

$$b = 1.77 \text{ in. (width of rectangular flat strip)}$$

$$c = 24 \text{ in.}$$

$$d = 0.3505 \text{ in.}$$

$$f_1 = 1.12 \text{ in.}$$

$$f_2 = 0.26 \text{ in.}$$

$$h = h_c + \frac{t_s}{2} = 1.202 \text{ in.}$$

$$h_c = 1.1860 \text{ in.}$$

$$p = 1.49 \text{ in.}$$

$$R = 0.346 \text{ in.}$$

$$t_s = t_c = 0.032 \text{ in.}$$

$$\theta = 79.13^\circ = 1.3811 \text{ rad}$$

Local Buckling—Elastically Supported

The experimental observations by R. Fields (ref. 7) and the finite-element buckling analysis (carried out by W. Percy of McDonnell Douglas, ref. 7) showed that the flat rectangular plate strip (fig. 2) would buckle with 13 buckle half-waves ($m = 13$) in the x -direction and 1 buckle half-wave ($n = 1$) in the y -direction (fig. 4). Thus, by taking $m = 13$, $n = 1$, equation (1) gives the buckling stress $(\sigma_x)_{cr}$ of the rectangular plate

$$(\sigma_x)_{cr} = 19,060 \text{ lb/in}^2$$

from which the panel buckling load $(N_x)_{cr}$ is calculated from equation (8) as

$$(N_x)_{cr} = 1600 \text{ lb/in}$$

which gives the buckling load of $P_{cr} = 38,400 \text{ lb}$.

Local Buckling—Simply Supported

For $m = 13$, $n = 1$, equation (10) gives

$$(\sigma_x)_{cr} = 19,068 \text{ lb/in}^2$$

which gives the value of the panel buckling load $(N_x)_{cr}$ (eq. (8)) as

$$(N_x)_{cr} = 1601 \text{ lb/in}^2$$

The compressive buckling load will then be $P_{cr} = 38,424 \text{ lb}$, which is slightly larger than the previous case.

Both of the previous two predictions are slightly lower than the buckling load of 39,700 lb calculated from finite-element buckling analysis and the measured value of 41,403 lb by Fields (ref. 7).

Global Buckling

The lowest buckling load for the global buckling will occur at $m = 1$ and $n = 1$. Thus, the panel buckling load calculated from equation (11) has the value of $k_x = 5.61$, which gives

$$(N_x)_{cr} = 4917 \text{ lb/in}$$

which gives the compressive buckling load of $P_{cr} = 108,008 \text{ lb}$. This load is approximately three times larger than the value predicted from local buckling analysis. Thus, the global buckling is unlikely to occur before the local buckling.

The following table summarizes the present results of the compressive buckling study.

Table 1. Comparison of compressive buckling loads.

Case	$(N_x)_{cr}$, lb/in	P_{cr} , lb
Local buckling:		
Elastically supported	1,600	38,400
Simply supported	1,601	38,424
Global buckling	4,500	108,008
W. Percy's finite element (ref. 7)	1,654	39,700
Fields' experiment (ref. 7)	1,725	41,403

The predicted local compressive buckling loads are slightly lower than the value predicted from Percy's finite-element buckling analysis, and are also lower than Field's experimental value. The reason may be the existence of the reinforcements at the test panel edges (fig. 4), which were neglected in the compressive buckling analysis.

CONCLUSION

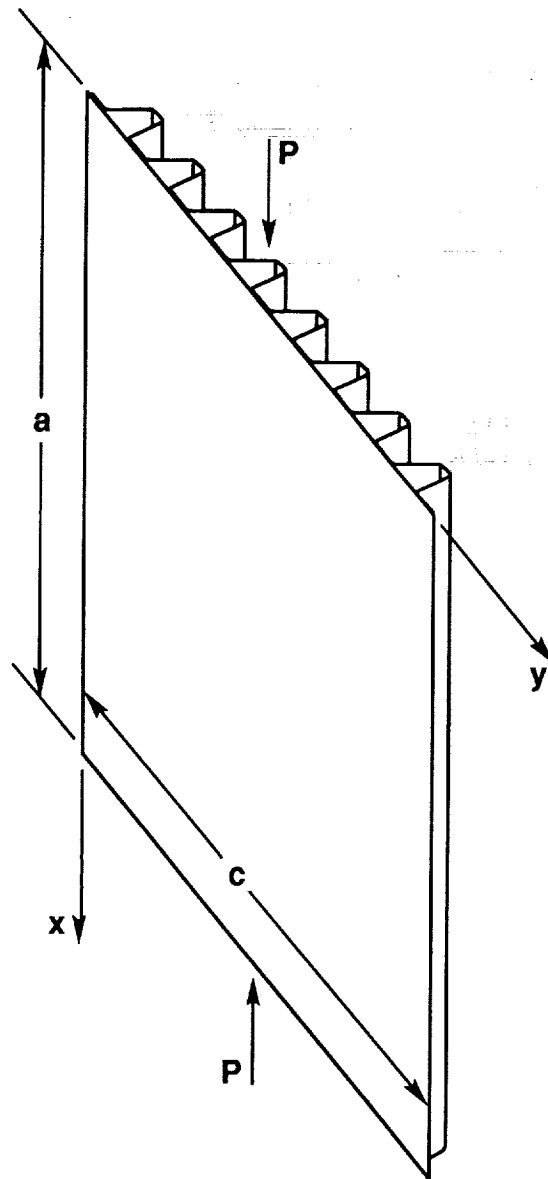
Compressive buckling behavior of a hat-stiffened panel was analyzed in the light of local bucklings and global buckling. The predicted compressive local buckling loads were slightly lower than the value predicted from finite-element buckling analysis and were also lower than the experimental value. The reason may be the existence of the reinforcements at the panel edges, which were ignored in the analysis.

The global buckling theory predicted the compressive buckling load approximately three times more than the values predicted from local buckling theories. Therefore, the hat-stiffened panel will buckle locally instead of globally.

*Dryden Flight Research Facility
National Aeronautics and Space Administration
Edwards, California, May 14, 1991*

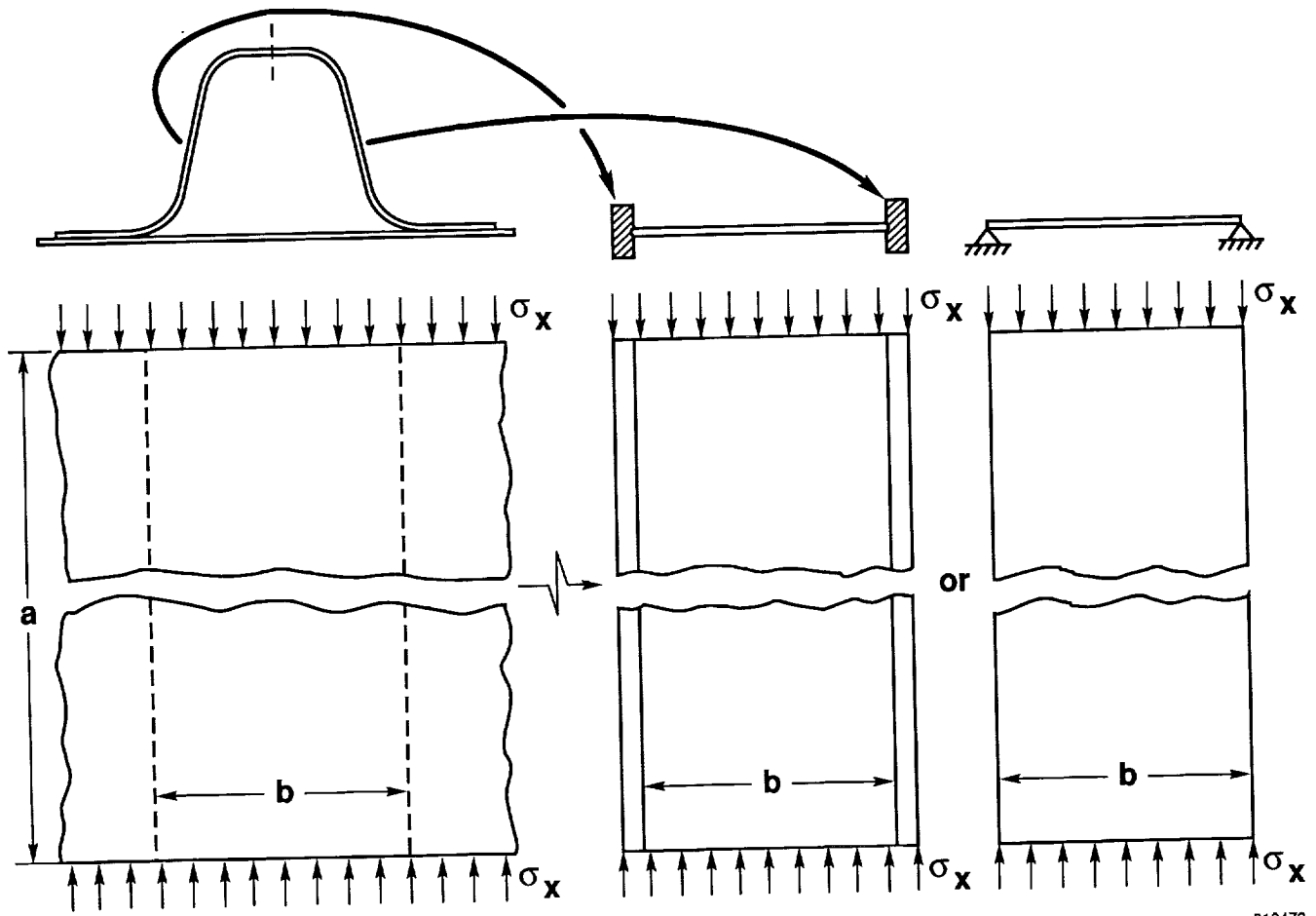
REFERENCES

1. Musgrove, Max D. and Bruce E. Greene, *Advanced Beaded and Tubular Structural Panels*, NASA CR-2514, 1975.
2. Siegel, William H., *Experimental and Finite Element Investigation of the Buckling Characteristics of a Beaded Skin Panel for a Hypersonic Aircraft*, NASA CR-144863, 1978.
3. Ko, William L., John L. Shideler, and Roger A. Fields, *Buckling Characteristics of Hypersonic Aircraft Wing Tubular Panels*, NASA TM-87756, 1986.
4. Ko, William L., "Elastic Stability of Superplastically Formed/Diffusion Bonded Orthogonally Corrugated Core Sandwich Plates," AIAA 80-0683, presented at the AIAA/ASME/ASCE/AHS 21st Structures, Structural Dynamics, and Materials Conference, Seattle, Washington, May 12-14, 1980.
5. Timoshenko, Stephen P., *Theory of Elastic Stability*, McGraw-Hill Book Co., New York, 1961.
6. Libove, Charles and Ralph E. Hubka, *Elastic Constants for Corrugated-Core Sandwich Plates*, NACA TN-2289, 1951.
7. Percy, W. and R. Fields, "Buckling Analysis and Test Correlation of Hat Stiffened Panels for Hypersonic Vehicles," AIAA 90-5219, presented at the AIAA Second International Aerospace Planes Conference, Orlando, Florida, Oct. 29-31, 1990.



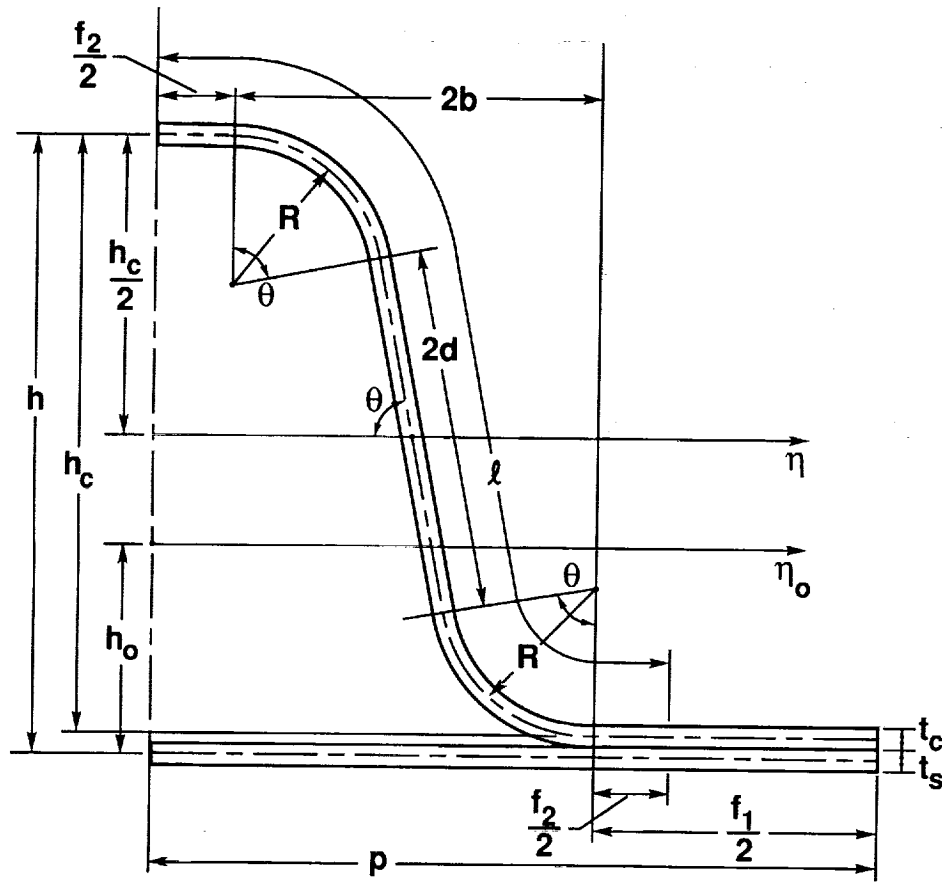
910471

Figure 1. Hat-stiffened panel under uniaxial compression.



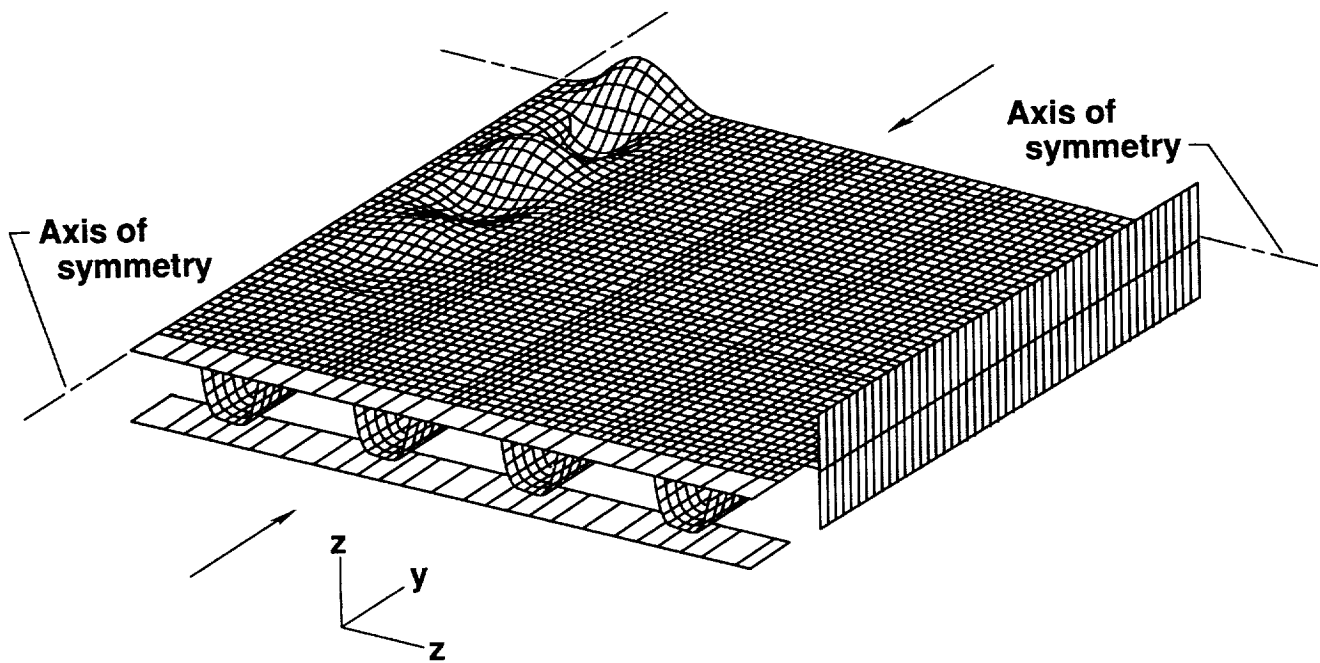
910472

Figure 2. Compressive buckling of hat-stiffened panel analyzed by using two simplified local models.



910473

Figure 3. Segment of hat-stiffened flat panel.



910474

Figure 4. Buckled shape of hat-stiffened panel under uniaxial compression. (Finite-element buckling analysis by W. Percy, McDonnell Douglas, ref. 7.)



Report Documentation Page

1. Report No. NASA TM-4310		2. Government Accession No.		3. Recipient's Catalog No.	
4. Title and Subtitle Compressive Buckling Analysis of Hat-Stiffened Panel				5. Report Date August 1991	
				6. Performing Organization Code	
7. Author(s) William L. Ko and Raymond H. Jackson				8. Performing Organization Report No. H-1724	
				10. Work Unit No. RTOP 505-63	
9. Performing Organization Name and Address NASA Dryden Flight Research Facility P.O. Box 273 Edwards, California 93523-0273				11. Contract or Grant No.	
				13. Type of Report and Period Covered Technical Memorandum	
12. Sponsoring Agency Name and Address National Aeronautics and Space Administration Washington, DC 20546-3191				14. Sponsoring Agency Code	
				15. Supplementary Notes	
16. Abstract <p>Buckling analysis was performed on a hat-stiffened panel subjected to uniaxial compression. Both local buckling and global buckling were analyzed. It was found that the global buckling load was several times higher than the local buckling load. The predicted local buckling loads compared favorably with both experimental data and finite-element analysis.</p>					
17. Key Words (Suggested by Author(s)) Compressive buckling Global buckling Hat-stiffened panel Local buckling			18. Distribution Statement Unclassified — Unlimited Subject category 39		
19. Security Classif. (of this report) Unclassified		20. Security Classif. (of this page) Unclassified		21. No. of Pages 16	22. Price A02